Asian Journal of Chemistry; Vol. 25, No. 2 (2013), 713-718

ASIAN JOURNAL OF CHEMISTRY

http://dx.doi.org/10.14233/ajchem.2013.12568

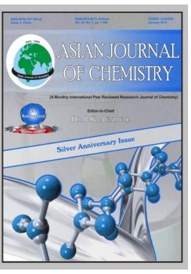

Enhancement of Photocatalytic Decolorization of Methylene Blue Over WO_3/CNT Incorporated TiO_2 Nanocatalysts Under UV Light Radiation

LEI ZHU[1], ZE-DA MENG[1], KWANG-YOUN CHO[2], TRISHA GHOSH[1] and WON-CHUN OH[1,*]

[1]Department of Advanced Materials Science & Engineering, Hanseo University, Chungnam 356-706, South Korea
[2]Korea Institute of Ceramic Engineering and Technology, Seoul 153-801, South Korea

*Corresponding author: Fax: +82 41 6883352; Tel: +82 41 6601337; E-mail: wc_oh@hanseo.ac.kr

(*Received*: 12 August 2011; *Accepted*: 14 August 2012) AJC-11962

The photodegradation of methylene blue solution catalyzed by anatase TiO_2 and composite photocatalysts: WO_3/TiO_2, $WO_3/CNT/TiO_2$ (with different content of W) was studied under irradiation with UV light. The catalysts were characterized by SEM, TEM, BET, XRD, EDX and UV-VIS absorption spectroscopy. The results showed that MWCNTs used as supports materials efficiently inhibit the agglomeration of WO_3/TiO_2 and improve the dispersion of nanoparticles. The photoactivity of the prepared materials under UV irradiation was tested using the conversion of methylene blue in aqueous solution. In comparison with non-nanocarbon supported WO_3/TiO_2 composites, the nanocarbon supported WO_3/TiO_2 composites had higher absorption ability with a larger specific surface area and showed higher photocatalytic activity of degradation methylene blue solution under UV light irradiation, meanwhile it was found that an optimal WO_3 dosage of 8.80 wt % in $WO_3/CNT/TiO_2$ composite achieved the highest photodegradation rate in this study. It can be considered that the methylene blue removal effect of the $WO_3/CNT/TiO_2$ composite is affected by two kinds of effects: adsorption effect by MWCNTs and photoctalytic effect by TiO_2. Finally, the reasons for the obvious increase of photocatalytic activity indicated that the effect of MWCNTs, which could absorb UV light to create photoinduced electrons (e^-) and the electron trapping effect of WO_3, which resulted in the recombination rate of electrons/holes in $WO_3/CNT/TiO_2$ declined.

Key Words: Tungsten oxide/MWCNTs, Titanium dioxide, Photocatalytic properties, UV light, Methylene blue.

INTRODUCTION

At present energy and environmental crisis is the very serious challenge of survival and development for modern humans. Environmental protection has attracted more and more attention through various approaches. Photocatalytic purification of water and air has been considered as one of the promising methods. Among many of the photocatalyst, TiO_2 is widely used as a most excellent photocatalyst due to its semiconductor characteristic, high photocatalytic activity, strong oxidation ability, low energy consumption, low cost, chemical stability and non-toxicity.

However, the use of TiO_2 as photocatalysts is limited mainly to the recombination of the generated photo-holes and photo-electrons. Photocatalysis involves the oxidation of a chemical by photo-holes from the semiconductor, so every recombination event involves the loss of holes that might otherwise have promoted degradation. Therefore, the major transfer of photogenerated electrons and holes between the valence and conduction bands of semiconductors is important to photocatalysis. Various methods have been reported to improve photocatalytic efficiency by the modification of surface or bulk properties, *i.e.*, doping, codeposition of metals, surface chelating, mixing of two semiconductors, coating of an insulating oxide layer, *etc.*[1-5].

The mechanism of coupled semiconductors is to increase the photocatalytic efficiency by increasing the charge separation and extending the photo-responding range. Now, the research about doping another semiconductor on the surface of TiO_2 includes SnO_2-TiO_2[6,7], V_2O_5-TiO_2[8], ZnO-TiO_2[9], ZrO_2-TiO_2[10,11], CdS-TiO_2[12]. Since WO_3 has a slightly lower conduction band than TiO_2, the photoelectrons are prone to transfer from the conduction band of TiO_2 to that of WO_3 and result in the effective charge carrier separation when TiO_2 nanotube array is coupled with WO_3[13-15]. It has been reported that TiO_2 nanotube arrays coupled with WO_3 possess enhanced electrochromic properties and a significantly lower threshold voltage[16]. Do *et al.*[17] found the degradation rate of 1,4-dichlorobenzene was enhanced by addition of WO_3 on the surface of TiO_2.

However, as other powder photocatalysts, WO_3/TiO_2 nanoparticles have some disadvantages, such as difficult recovery, easy cohesion and low utilization rate in practical applications. Some alternative methods are immobilizing nanoparticles onto an inert and porous supporting matrix; through the accumulation of carriers the adsorption mass transfer rate and efficiency of photocatalytic degradation are effectively improved[18-21]. As a good support for nanomaterials, multi-walled carbon nanotubes (MWCNTs) efforts have been made to explore their applications using various approaches since the discovery by Iijima[22], as they are in fact one of the most remarkable emergent materials. In a recent review, attention has been drawn to the fact that CNT can compete with activated carbon as catalyst supports and peculiar behaviours in terms of conversion or selectivity, which were attributed to the combination of their electronic, specific active-phase-support interaction, adsorption, mechanical and thermal properties[23].

Because of their great hardness and toughness, CNT maintain their morphology and structure even at high nanoparticle loadings. In past, a variety of metal oxides, such as GeO_2, Eu_2O_3, V_2O_5, ZnO, RuO_2, *etc*., have been decorated to the surface of CNTs by some research groups[24-28]. The combination of CNTs with metal oxide nanoparticles can be used as catalysts, sensors, semiconductor devices, data storage/processing devices and new reinforced nanofiber materials[29].

In consideration of the basic disadvantage of WO_3 as a photocatalyst which has a low photonic efficiency. In this report, we combined both advantage of introducing MWCNT and WO_3, successfully fabricated a novel photocatalyst through the method of sol-gel-dipping-calcination with the aim of: (i) determine the decolorization efficiency of methylene blue at various reaction times for different samples; (ii) elucidate the effects of WO_3 on decolorization effiency; (iii) enhance the step of the application of the technology of nano particulate TiO_2 photodegradation and improving the particle size distribution structure; (iv) establish the prevenient dye-photodegradation mechanisms using WO_3/CNT/TiO_2 composites.

EXPERIMENTAL

The ammonium metatungstate hydrate ($H_{26}N_6O_{40}W_{12}\cdot xH_2O$) purchased from Sigma-AldrichTM Chemie GmbH (Germany) was used as raw material to decomposition generate WO_3 at high temperature. The titanium(IV) *n*-butoxide (TNB, $C_{16}H_{36}O_4Ti$) as a titanium source for the preparation of the WO_3/CNT/TiO_2 composites was purchased as reagent-grade from Acros Organics (USA). MWCNTs (95.5 %) powder with diameter of 20 nm and length of 5 μm was purchased from Carbon Nano-material Technology Co. Ltd., Korea. For the oxidization the surface of MWCNTs, MCPBA (*m*-chloroperbenzoic acid) was used as an oxidizing reagent purchased from Acros Organics, New Jersey, USA. Benzene (99.5 %) and ethyl alcohol were purchased as reagent-grade from Duksan Pure Chemical Co. (Korea) and Daejung Chemical Co. (Korea) and used without further purification unless otherwise stated. Methylene blue ($C_{16}H_{18}N_3SCl\cdot 3H_2O$) was analytical grade and also purchased from Duksan Pure Chemical Co. Ltd. (Korea).

Synthesis of WO_3/CNT/TiO_2 photocatalyst: For designing an effective photocatalyst (WO_3/CNT/TiO_2), we used a new synthesize process. As is well-known, the MWCNT is so stable that it needs to be treated with strong acids to introduce active function groups on their surface for many applications. Thus 2 g of *m*-chloroperbenzoic acid was dissolved in 80 mL benzene and then 1 g CNT powder was put into the oxidizing agent solution, refluxed at 353 K for 6 h then the solid precipitates were formed and dried at 363 K. Then the treated MWCNTs were milled and washed with distilled water and ethanol and dried at 333 K in vacuum.

In order to synthesize three kinds of WO_3/CNT compounds, different contents of $H_{26}N_6O_{40}W_{12}\cdot xH_2O$ powder was added to 60 mL of water in three breakers, respectively and stirred until they were completely dissolved. Further 0.3 g of oxidized CNT was taken out and added to this mixture separately and stirred magnetically at 353 K. After reaction for 10 h, the formed gels were refluxed at 373 K for 8 h and then heat treatment at 773 K for 1 h with a heating rate of 279 K/min. Finally, three kinds of WO_3/CNT composites were obtained and named WC1, WC2, WC3.

On the other hand, 4 mL of titanium *n*-butoxide was dissolved in 80mL of benzene to get the sol. The WC1, WC2, WC3 composites was put into the sol, after homogenized at 353 K for 8 h using a shaking water bath (Lab house, Korea) with a shaking rate of 120 rpm/min, the WO_3/CNT/TiO_2 gels were obtained. The WO_3/CNT/TiO_2 gels were heat treated at 773 K for 1 h to form the WO_3/CNT/TiO_2 photocatalysts which named WCT 1, WCT 2, WCT 3. The procedure of prepared samples is shown in Fig. 1. The preparation conditions and the sample code used in this study were listed in Table-1.

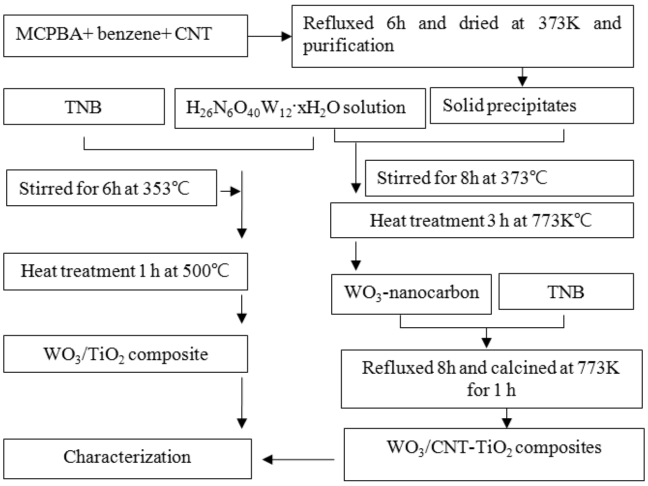

Fig. 1. Preparatory procedure of WO_3/TiO_2 and WO_3/CNT/TiO_2 composite

TABLE-1
NOMENCLATURES OF SAMPLES PREPARED WITH WO_3/TiO_2 AND WO_3/CNT/TiO_2 COMPOSITE

Preparation method	Nomenclatures
$H_{26}N_6O_{40}W_{12}\cdot xH_2O$ + benzene + TNB	WT
Oxidized CNT + $H_{26}N_6O_{40}W_{12}\cdot xH_2O$ 1 + 2 mL TNB	WCT1
Oxidized CNT + $H_{26}N_6O_{40}W_{12}\cdot xH_2O$ 2 + 2 mL TNB	WCT2
Oxidized CNT + $H_{26}N_6O_{40}W_{12}\cdot xH_2O$ 3 + 2 mL TNB	WCT3

TNB = Titanium *n*-butoxide

For comparison and verification the photocatalytic effect of WO_3/TiO_2, the composite was performed by titanium *n*-butoxide as TiO_2 source with a solution of $H_{26}N_6O_{40}W_{12}\cdot xH_2O$ by a sol-gel method. Some amount of $H_{26}N_6O_{40}W_{12}\cdot xH_2O$

powder dissolved in very little amount of distilled water and 50 mL of benzene was added to it under continuous stirring. Further 4 mL TNB was added to the solvent under magnetic stirring for 8 h at 353 K. The obtained mixture was dried at 373 K for 5 h and calcined at 773 K for 1 h.

Characterization of catalysts: SEM (scanning electrion microcopy, JSM-5200 JOEL, Japan) was used to observe the morphology and microstructure of WO_3 modified TiO_2 and the samples of MWCNTs introduced WO_3/CNT /TiO_2 composites with increased content of W.

Transmission electron microscopy (TEM, JEOL, JEM-2010, Japan) at an acceleration voltage of 200 kV was used to investigate the size and distribution of the WO_3 and TiO_2 deposits on the MWCNTs surface of various samples. TEM specimens were prepared by placing a few drops of the sample solution on a carbon grid.

For the determination of the crystallographic structure of the inorganic constituent of the composites, X-ray diffraction analysis (XRD) was taken using an X-ray generator (Shimadzu XD-D1, Japan) with CuK_α irradiation (0.154056 nm) at room temperature. The nature of the phase in the sample was checked using the database of the Joint Committee on Powder Diffraction Standards (JCPDS).

EDX spectra were also used for the elemental analysis of the samples. The Brunauer-Emett-Teller (BET) surface area of these photocatalyst composite was determined by N_2 adsorption measured at 77 K using a BET analyzer (Monosorb, USA). For the analysis of photo-degradation effects, UV-VIS adsorption parameters for the WT, WCT1, WCT 2, WCT 3 composites were recorded by a UV-VIS (Optizen Pop Mecasys Co., Ltd., Korean) spectrophotometer.

Determination of photocatalytic properties: Photocatalytic activities were evaluated by methylene blue degradation in aqueous medium at ambient temperature under ultraviolet light irradiation with a wavelength of 365 nm and 20 W output. The UV lamp was used at the distance of 100 mm from the solution in darkness box. The initial methylene blue concentration (c_0) was 1.0×10^{-5} mol/L. And the amount of photocatalyst composites was keep at 10 mg. Before turning on illumination, the suspension solution containing 50 mL of methylene blue and the photocatalyst composites was placed for 2 h in the darkness box to establish an adsorption-desorption equilibrium. Experiments were then carried out under UV light. Solution was withdrawn regularly from the reactor by an order of 30, 60, 90 and 120 min and immediately centrifuged to separate any suspended solid. The clean transparent solution was analyzed by using a UV-VIS spectrophotometer. Then, the full spectrum (200-750 nm) of each sample was recorded and the characteristic absorption of methylene blue at 665 nm was chosen as the monitored parameter for the photocatalytic degradation process.

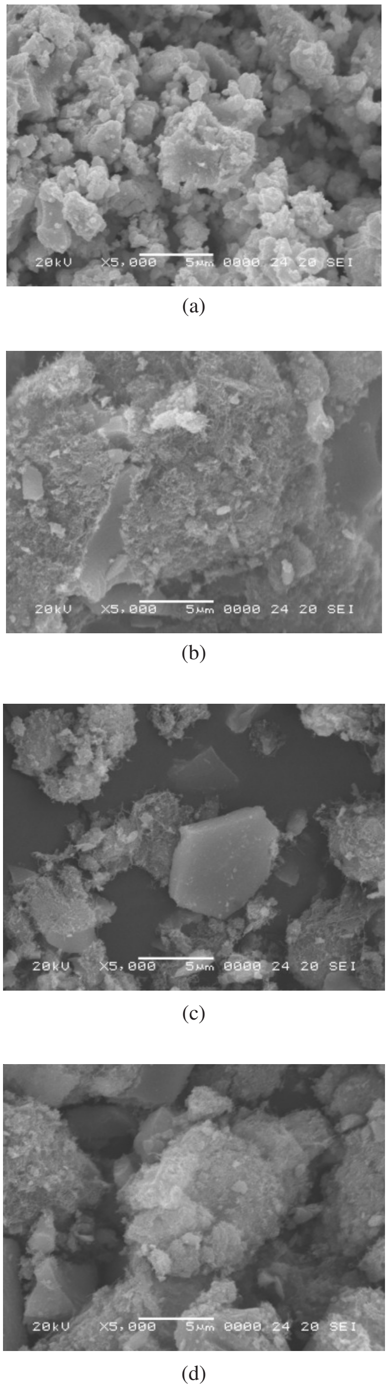

(a)

(b)

(c)

(d)

Fig. 2. SEM micrographs of WO_3/TiO_2 and WO_3/CNT/TiO_2 composites: (a) WT, (b) WCT1, (c) WCT2, (d) WCT3

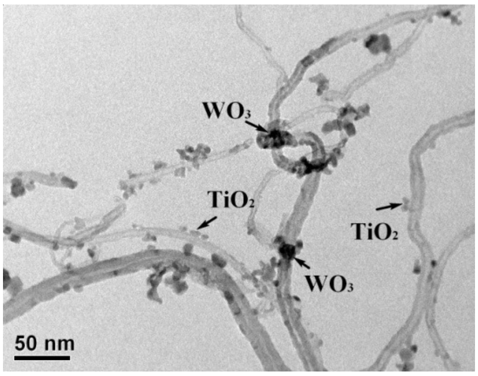

(a)

RESULTS AND DISCUSSION

SEM and TEM analysis: The typical micro-surface structures and morphology of the WT and WCT composites were characterized by SEM (Fig. 2) and TEM (Fig. 3). Fig. 2 shows the macroscopical changes in the morphology of WT and WCT. As shown in Fig. 2(a), TiO_2 and WO_3 were agglomerated with

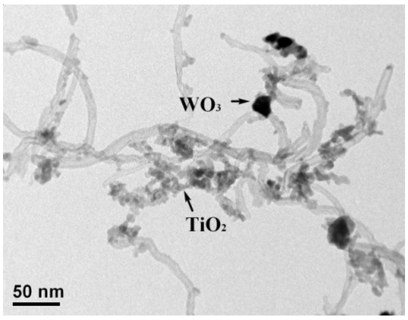

(b)

Fig. 3. TEM micrographs of WO_3/CNT/TiO_2 composite: (a) WCT1, (b) WCT3

each other thus we could not find the exact crystal morphology, it can be attributed that when the crystal particle size is very small, it can easily agglomerate due to the weak forces of the surface. From Fig. 2(b-d), the porous structure can be observed and the TiO_2 agglomerate is coated on the WO_3/CNT composite. However, small amounts of TiO_2 particles were also aggregated to be bundles, which possibly are not well homogenized during vigorous stirring. It was considered that better dispersion enables larger number of active catalytic centers for the photocatalytic reaction[30]. These results are also confirmed by TEM inspection of the WO_3/CNT/TiO_2 composite. As shown in Fig. 3, for the WO_3/CNT/TiO_2 composite, the TiO_2 particles were distributed uniformly outside surface of CNT tube, WO_3 particles were completely attached on the surface of the tube this caused partial agglomeration to form blocky-shaped particle. Most of the WO_3 was in the quasi-spherical shape, *ca.* 5-15 nm in size, coating the outside surface of the MWCNT, very few isolated WO_3 particles were observed. The average size of the TiO_2 particles was smaller than that of the WO_3 particles. Therefore, the higher photocatalytic activity of the WO_3/CNT/TiO_2 composite might be attributed to the small and nano-sized distribution of titanium complexes including titanium dioxide, the energy sensitizer for improving the quantum efficiency and an increase of charge transfer of the MWCNTs.

BET surface area analysis: The values of the BET surface area of CNT, WT, WCT 1, WCT 2, WCT 3 samples are presented in Table-2. The BET surface area of CNT and WO_3/TiO_2 were 211.43 and 38.44 m^2/g. The BET surface areas of WCT 1, WCT 2, WCT 3 were 93.64, 101.43 and 99.13 m^2/g, respectively. It is clearly shown that the agglomeration is caused easily in the process of WO_3/TiO_2 preparation because of its higher surface energy. When CNT was introduced in WO_3/TiO_2 composite, it can prevent TiO_2 particles and WO_3 particles form agglomerating, thus there was large change of the micro-pore size distribution for WO_3/CNT/TiO_2 composite compared to that of corresponding WO_3/TiO_2. This indicated that the supported CNT was directly related to adsorption ability of TiO_2.

TABLE-2
BET SURFACE AREA OF WO_3/CNT/TiO_2 COMPOSITE

Samples	S_{BET} (m^2/g)
Original MWCNT	211.43
WT	38.44
WCT1	93.64
WCT2	101.43
WCT3	99.13

XRD analysis: The XRD analysis results for the catalysts are shown in Fig. 4. Diffraction peaks corresponding to anatase are marked with 'A'; diffraction peaks corresponding to the WO_3 phase are marked with 'W'. In the XRD patterns for the carbon nanotube non-treated WT composite, the diffraction peaks of tungsten oxide were certainly observed because of the high tungsten content and high crystallinity. The sharp peaks corresponding to 23.2, 24.5, 28.3, 34.1 and 36.8° 2θ were indicative of monoclinic WO_3[31] increasing with the W content. For the WCT composites, the major peaks at 25.3, 37.8, 48.0, 53.8, 54.9 and 62.5° 2θ were assigned to diffraction planes of (101), (004), (200), (105), (211) and (204) of anatase, indicating the prepared WCT composite existed as anatase. One broad peaks are measured at 2θ values of approximately 25.80°. It's the characteristic peaks corresponding to the MWCNTs molecular crystal structure. These peaks correspond to d-values of 0.345 nm[32]. MWCNTs and one of titanium characteristic peaks are overlap at around 25.0°, so intensity of the peak is increased.

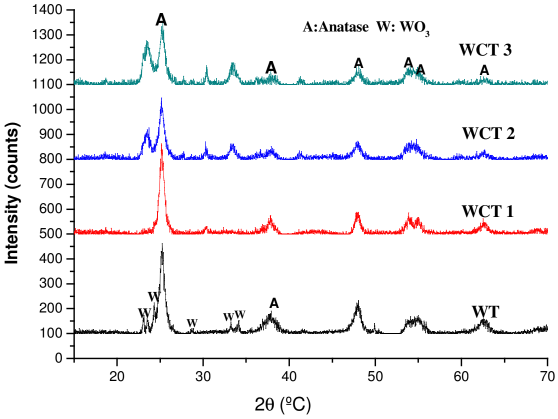

Fig. 4. XRD analysis of WO_3/TiO_2 and WO_3/CNT/TiO_2 composite

EDX analysis: The quantitative microanalysis of C, O, Ti and W as major elements for the WO_3/TiO_2 and WO_3/CNT/TiO_2 composites was performed by EDX. The EDX spectra of the WO_3/TiO_2 and WO_3/CNT/TiO_2 composites are shown in Fig. 5. The results of the EDX elemental microanalysis of the WO_3/TiO_2 and WO_3/CNT/TiO_2 composites were listed in Table-3. From the EDX data, the main elements such as C, O, Ti and W existed. The contents of the tungsten component for WT, WCT 1, WCT 2 and WCT 3 are 61.57, 5.48, 8.8 and 11.15 %, respectively. It can be expected that the contents of the tungsten component in the composites increased with an increase of WO_3 concentrations. In case of most of the samples, carbon and titanium were present as major elements with small quantities of oxygen in the composite.

TABLE-3
EDX ELEMENTAL MICROANALYSIS OF
WO_3/TiO_2 AND WO_3/CNT/TiO_2 COMPOSITE

Samples	Elements (wt %)			
	C	O	Ti	W
WT	0	26.51	11.92	61.57
WCT1	33.95	28.49	32.08	5.48
WCT2	37.21	22.86	31.13	8.80
WCT3	28.59	28.10	32.17	11.15

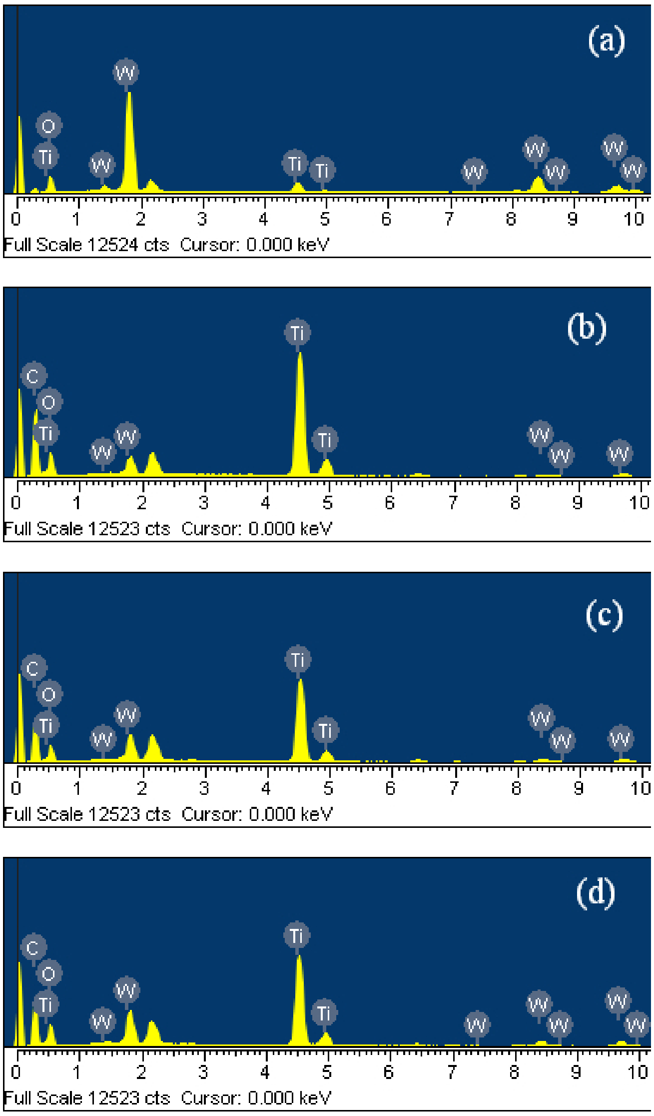

Fig. 5. EDX analysis of WO$_3$/TiO$_2$ and WO$_3$/CNT/TiO$_2$ composite: (a) WT, (b) WCT1, (c) WCT2, (d) WCT3

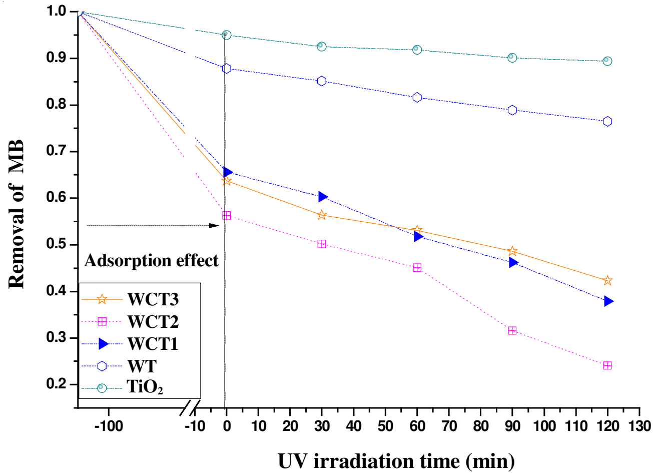

Fig. 6. Removal of the methylene blue solution by pure TiO$_2$, WO$_3$/TiO$_2$, WO$_3$/CNT/TiO$_2$ composites

Photocatalytic degradation of methylene blue: The adsorption abilities and photodegradation efficiency of pure TiO$_2$, WT, WCT 1, WCT 2 and WCT 3 composites evaluated with 2 h placed in the dark box and excitated UV light were shown in Fig. 6. It was quite easy to draw a causal relationship between surface areas in Table-2. It was clear that adsorption abilities of methylene blue on WCT samples were faster than that of pure TiO$_2$ powder. This was attributed to the high porosity of the WCT surface due to introduction of porous carbon material- MWCNTs, which correlated with an increase in adsorption ability.

In Fig. 6 it also shown that for degradation of methylene blue solution the photocatalytic activity of WT was higher than that of the pure TiO$_2$ but the WCT photocatalyst exhibited an excellent photocatalytic activity of three kinds of samples. However, for WCT 1, WCT 2 and WCT 3 these three kinds of photocatalyst, with increasing the content of W, the photocatalytic efficiency was not correspond to the increase. The WCT 2 sample with W content of 8.80 % shown the best photocatalytic decolorization ability of methylene blue solution, it can be considered that using a larger amount of WO$_3$ as dopant, on the contrary the WO$_3$ was easy to be the recombination center of electron-hole pairs which results that decrease the photocatalytic efficiency.

As mentioned above, to increase the efficiency of the photodegradation of dye, we may increase the amount of electron (e$^-$) and prevent the recombination of the electron-hole. As studies, MWCNTs had an energy sensitizer for improving the quantum efficiency and an increase of charge transfer. It is believed that the high efficiency degradation of methylene blue concentration in the aqueous solution can be occurred in three physical phenomena such as from the quantum efficiency of the MWCNTs, photogenerated electrons trap effect of WO$_3$ and photocatalytic decomposition by TiO$_2$. methylene blue molecules absorb energy from irradiation, thereby shifting their delocalized electrons from bonding to antibonding orbitals. Since methylene blue adsorption likely occurs *via* π-π interactions between its delocalized electrons and the graphene layers of carbon, it is reasonable that shifts in its electron orbitals would alter adsorption. It is considered that the TiO$_2$ deposited on the MWCNTs surface can retain its photo-degradation activity.

The tungsten oxide dopant in the titania crystalline matrix can prevent the recombination which promotes the efficiency of TiO$_2$. Furthermore, when the WO$_3$/CNT/TiO$_2$ composite was irradiated with UV light, according to some studies under UV light irradiation, the MWCNT can absorb UV light to create photo-induced electrons (e$^-$) into the conduction band (CB) of the TiO$_2$ particles with increasing amount of electrons[33,34]. And the essence of the charge separation mechanism in the WO$_3$-TiO$_2$ composite consists in electron transfer from the conduction band of TiO$_2$ to WO$_3$ conduction band, accompanied by consecutive W^{6+} reduction into W^{5+}, occurring on the surface of the WO$_3$ crystal lattice[35]. The electron transfer from the photoactive TiO$_2$ to WO$_3$ leads to an increase in the lifetime of the photogenerated pairs and as a consequence to a promotion of the photonic efficiency of the photocatalytic degradation of organic substrates. On the other hand, the photogenerated holes remain on the WO$_3$ particles and TiO$_2$ particles theoretically migrate to the surface and react with OH$^-$ or H$_2$O to generate OH$^\bullet$ and the electrons trapped on WO$_3$ can react with molecular O$_2$ to form O$_2^\bullet$-radicals, which eventually oxidize methylene blue, the reactions can be expressed as follows:

$$WO_3/TiO_2 + h\nu \rightarrow WO_3\ (h^+, e^-)/TiO_2 \quad (1)$$

$$WO_3(h^+, e^-)/TiO_2 \rightarrow WO_3(e^-)/TiO_2(h_{VB}^+) \quad (2)$$

$$e^- + O_2 \rightarrow O_2^{\bullet -} \quad (3)$$

$$h^+ + OH^- \rightarrow OH^\bullet \quad (4)$$

$$h^+ + H_2O \rightarrow OH^\bullet + h^+ \quad (5)$$

And the reaction mechanism of the $WO_3/CNT/TiO_2$ composite under UV light irradiation was shown in Fig. 7.

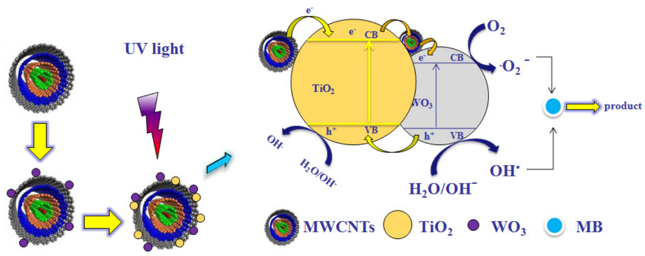

Fig. 7. Schematic diagram of the mechanism of preparation and photocatalytic activity of the $WO_3/CNT/TiO_2$ composite

Conclusion

The new photocatalyst composites of $WO_3/CNT/TiO_2$ was prepared by the sol-gel method and its chemical composition and optical absorption were examined by SEM, TEM, XRD, BET and UV-VIS adsorption spectra. The surface are of all the composites is less than that of pristine MWCNTs and compared with WO_3/TiO_2 the surface area was increased after introduction of MWCNTs. According to the TEM images, TiO_2 particles are uniformly dispersed on the surface of MWCNTs with several WO_3 particles between them in case of $WO_3/CNT/TiO_2$ composites. And the size of TiO_2 and WO_3 particles is about 5-15 nm. Finally, the photoactivity of the prepared materials, under UV irradiation, was tested using the conversion of methylene blue from model aqueous solution. The higher efficiency of photo-decolorization of the substrate catalyzed by $WO_3/CNT/TiO_2$ in comparison to anatase TiO_2 can be attributed to the more efficient separation of surface charge carriers in the WO_3/TiO_2 photocatalyst and to an increase in the quantity of generated $HO^\bullet$ radicals on the valence bands of WO_3 and TiO_2, comprised by the composite photocatalyst as a result of the better adsorption of H_2O and $HO^\bullet$ on its surface. On the other hand, the higher activity of photocatalytic destruction of methylene blue in the case of nanosized MWCNTs as support material coated with WO_3 and TiO_2 particles is owing to increase in the lifetime of the charge carriers and enhancement of the efficiency of the interfacial charge transfer to adsorbed substrates. Especially efficient is the charge separation in the case of the $WO_3/CNT/TiO_2$ photocatalyst during irradiation with UV light, when the optimal WO_3 dosage was 8.80 wt % its photo-decolorization efficiency was higher than that of the process catalyzed by WO_3/TiO_2 and achieved the highest photodegradation rate in this study.

REFERENCES

1. P.V. Kamat, *Chem. Rev.*, **93**, 267 (1993).
2. W.C. Oh, F.J. Zhang and M.L.Chen, *J. Ind. Eng. Chem.*, **16**, 299 (2010).
3. W.C. Oh, *J. Photocatal. Sci.*, **1**, 29 (2010).
4. H. Park and W. Choi, *J. Phys. Chem. B*, **108**, 4086 (2004).
5. P.V. Kamat, *J. Phys. Chem. B*, **106**, 7729 (2002).
6. L.R. Hou, C.Z. Yuan and Y. Peng, *J. Hazard. Mater.*, **139**, 310 (2007).
7. H. Ohsaki, N. Kanai, Y. Fukunaga, M. Suzuki, T. Watanabe and K. Hashimoto, *Thin Solid Films*, **502**, 138 (2006).
8. K.S. Chung, Z.D. Jiang, B.S. Gill and J.S. Chung, *Appl. Catal. A*, **237**, 81 (2002).
9. C.A.K. Gouvêa, F. Wypych, S.G. Moraes, N. Durán, N. Nagata and P. Peralta-Zamora, *Chemosphere*, **40**, 433 (2000).
10. D. Das, H.K. Mishra, K.M. Parida and A.K. Dalai, *J. Mol. Catal. A*, **189**, 271 (2002).
11. A. Kitiyanan, S. Sakulkhaemaruethai, Y. Suzuki and S. Yoshikawa, *Compos. Sci. Technol.*, **66**, 1259 (2006).
12. M.G. Kang, H.E. Han and K.J. Kim, *J. Photochem. Photobiol. A*, **125**, 119 (1999).
13. X.Z. Li, F.B. Li, C.L. Yang and W.K. Ge, *J. Photochem. Photobiol. A* , **141**, 209 (2001).
14. H.M. Yang, R.R. Shi, K. Zhang, Y.H. Hu, A.D. Tang and X.W. Li, *J. Alloys Compd.*, **398**, 200 (2005).
15. H.J. Liu, T.Y. Peng, D.N. Ke, Z.G. Peng and C.H. Yan, *Mater. Chem. Phys.*, **104**, 377 (2007).
16. A. Benoit, I. Paramasivam, Y.C. Nah, P. Roy and P. Schmuki, *Electrochem. Commun.*, **11**, 728 (2009).
17. Y.R. Do, K. Lee, K. Dwight and A. Wold, *J. Solid State Chem.*, **108**, 198 (1994).
18. Z. Ding, X.J. Hu, P.L. Yue, G.Q. Lua and P.F. Greenfield, *Catal. Today*, **68**, 173 (2001).
19. Y. Xu, W. Zheng and W. Liu, *J. Photochem. Photobiol. A*, **122**, 57 (1999).
20. A. Bhattacharyya, S. Kawi and M.B. Ray, *Catal. Today*, **98**, 431 (2004).
21. W.H. Leng, H. Liu, S.A. Cheng, J.Q. Zhang and C.N. Cao, *J. Photochem. Photobiol. A*, **131**, 125 (2000).
22. S. Iijima, *Nature*, **354**, 56 (1991).
23. P. Serp, M. Corrias and P. Kalck, *Appl. Catal. A*, **253**, 337 (2003).
24. Y.J. Zhang, J. Zhu, Q. Zhang, Y.J. Yan, N.L. Wang and X.Z. Zhang, *Chem. Phys. Lett.*, **317**, 504 (2000).
25. H.P. Yang, D.S. Zhang, L.Y. Shi and J.H. Fang, *Acta Mater.*, **56**, 955 (2008).
26. P.M. Ajayan, O. Stephan, P. Redlich and C. Colliex, *Nature*, **375**, 564 (1995).
27. J. Khanderi, R.C. Hoffmann, A. Gurlo and J.J. Schneider, *J. Mater. Chem.*, **19**, 5039 (2009).
28. Y.S. Min, E.J. Bae, K.S. Jeong, Y.J. Cho, J.H. Lee, W.B. Choi and G.S. Park, *Adv. Mater.*, **15**, 1019 (2003).
29. L. Fu, Z.M. Liu, Y.Q. Liu, B.X. Han, J.Q. Wang, P.G. Hu, L.C. Cao and D.B. Zhu, *Adv. Mater.*, **16**, 350 (2004).
30. M. Olek, T. Busgen, M. Hilgendorff and M. Giersig, *J. Phys. Chem. B*, **110**, 12901 (2006).
31. B. Pietruszka, F.D. Gregorio, N. Keller and V. Keller, *Catal. Today*, **94**, 102 (2005).
32. M. Drees, K. Premaratne, W. Graupner and J.R. Heflin, *Appl. Phys. Lett.*, **81**, 4607 (2002).
33. W.C. Oh and M.L. Chen, *Bull. Korean Chem. Soc.*, **29**, 159 (2008).
34. M.L. Chen, F.J. Zhang and W.C. Oh, *J. Korean Ceram. Soc.*, **45**, 651 (2008).
35. V. Keller, P. Bernhardt and F. Garin, *J. Catal.*, **215**, 129 (2003).